2016

Experimental Investigations of Low-temperature Driven Ejector for Isobutane

Mark Bergander
Magnetic Development, Inc, Madison, CT, USA, mark@mdienergy.com

Dariusz Butrymowicz
Bialystok University of Technology, Bialystok, 15-351, Poland, nd.butrymowicz@pb.edu.pl

Kamil Smierciew
Bialystok University of Technology, Bialystok, 15-351, Poland, k.smierciew@pb.edu.pl

Jerzy Gagan
Bialystok University of Technology, Bialystok, 15-351, Poland, j.gagan@pb.edu.pl

Sarken D. Kapayeva
Eastern Kazakhstan Technical University, Ust Kamenogorsk, Kaz, kapaewa_s@rambler.ru

Experimental Investigations of Low-Temperature Driven Ejector for Isobutane

Mark J. BERGANDER[1]*, Dariusz BUTRYMOWICZ[2], Kamil ŚMIERCIEW[2], JerzyGAGAN[2], Sarken D. KAPAYEVA[3]

[1]Magnetic Development, Inc,
Madison, CT, USA, mark@mdienergy.com

[2]Bialystok University of Technology
Bialystok, Poland, d.butrymowicz@pb.edu.pl

[3]Eastern Kazakhstan Technical University
Ust Kamenogorsk, Kazakhstan, kapaewa_s@rambler.ru

*Corresponding Author

ABSTRACT

The paper describes experimental and numerical investigation of ejection refrigeration system dedicated for short time storage of food products for local retail market, especially in rural areas. The work was sponsored by US Dept. of Agriculture under Phase I SBIR program. This novel method does not use electricity from the power grid and is cleaner for the environment than other refrigeration techniques. One of major problems in the retail market of perishable foodstuff is a lack of efficient refrigerated storage capacity. Existing technologies in most cases use conventional refrigeration systems that consume a large amount of electricity and use harmful working substances - usually harmful Freons, with high greenhouse effect and ozone depletion potential. In addition, ensuring the stability of the product temperature and humidity may be a challenge for most of the existing short time storage refrigerators. Responding to these challenges authors describe a new, ejector based refrigeration system that 1) utilizes solar or waste heat (below 100°C temperature) as a main source of energy, 2) eliminates the mechanical compressor, which is a main user of electricity and the main contributor to maintenance and reliability issues in cooling systems and 3) operates without any ozone depletion effects and any greenhouse gas emissions, when used with natural refrigerants. Until recently, ejector use in refrigeration systems was considered as controversial because most of the research conducted in the past has yielded only theoretical results without visible, commercial products. The main issue was a relatively low value of coefficient of performance (COP) in comparison with classical compression systems. Selection of the working fluid is the crucial problem because the system efficiency is strongly influenced by the thermodynamic properties of the refrigerant. It was found that the maximum efficiency was achieved with natural refrigerants, of which isobutane is the most favorable. However, primarily due to its flammable nature, it is not currently allowed in commercial systems in USA and Canada although it has been used for many years in all domestic refrigerators in Germany and other EU countries. For US market, two other environmentally friendly equivalents to isobutene were identified: R245fa and R1234ze both with zero ozone depletion potential.
The research described here had overcome another limitation - a lack of appropriate methods for the design of ejector geometry. Such methodology was developed and tested in a variety of thermodynamic cycles for cooling, heating and heat pumps. The test stand and the experimental results of investigation for isobutane as a working fluid along with CFD modeling results are shown and discussed in the paper in details.

1. INTRODUCTION

One of the crucial problems in retail market of perishable foodstuff is a lack of efficient and appropriate refrigerated storage capacity for short time storage of food products. Existing refrigeration technologies contribute to environment pollution, consume a large amount of electricity and in general are expensive and in many cases even

unaffordable to a small rural, retail business. Also, ensuring the required storage conditions in terms of the stability of the product temperature and humidity may be thought as a challenge for most of the existing short time storage refrigerators. The above is the reason for large amount of losses of the perishable foodstuff under retail market conditions, especially in rural areas.

The technology for refrigerated storage presented in this paper may be applied even in areas without access to electricity so it may provide an attractive solution to protect agricultural production from diseases and pests. It maybe considered as a step towards better food accessibility to vulnerable populations as well as to increase shelf life of many food products. It will have especially broad application for cooling in the field before the product is shipped to the market or storage warehouse (this is often referred to as "precooling"). Some highly perishable products such as broccoli, ripe tomatoes, carrots, leafy vegetables, strawberries, peaches, and plums must be cooled as soon as possible after harvesting and therefore filed refrigeration becomes an utmost importance.

The fundamental condition for good storage of most vegetables and fruits is to keep them in a steady state temperature. According to van Hoff law, lowering of vegetables temperature slows down the life activity of stored vegetables and fruits including breathing. Another important factor having impact on quality of vegetables is humidity of air. Only a few percent of vegetable and fruit mass is called dry matter and the rest is water. This is the reason why most of vegetables lose very easily moisture if they are kept in too dry air. Some of the foodstuff requires moderate storage conditions for short time storage in retail market, e.g. temperature/relative humidity+5 - +12°C / 85÷90% (Gross et al, 2002, Mazza, 1989). However, without access to the appropriate storage equipment e.g. cooling chambers, the quality of the food products strongly decreases (Mizera and Butrymowicz, 2011). It is important to note that fresh-cut fruit products for both retail and food service applications have increasingly appeared in the market place recently. In the coming years, it is commonly perceived that the fresh cut fruit industry will have unprecedented growth. The difficulties encountered with fresh cut fruit require a new and higher level of technical and operational sophistication.

In this paper, a solar-powered cooling system is considered for small-to-medium size warehousing facilities, capable for cooling and cold storage of agricultural products that require moderate temperature range, i.e. 4÷15 °C. This includes a wide variety of fruits and vegetables, eggs, milk and diary products, baked products, etc. It is expected that a line of refrigeration units will be developed and manufactured in various sizes, i.e. from 1 to 5 tons of refrigeration. The schematic and a corresponding p-h graph for this thermodynamic cycle is shown in Fig. 1. The ejection refrigeration system is applied in the solar cooling chamber. The ejection system is a fully thermal driven system therefore either solar or waste heat with temperatures well below 100°C can be utilized as energy source.

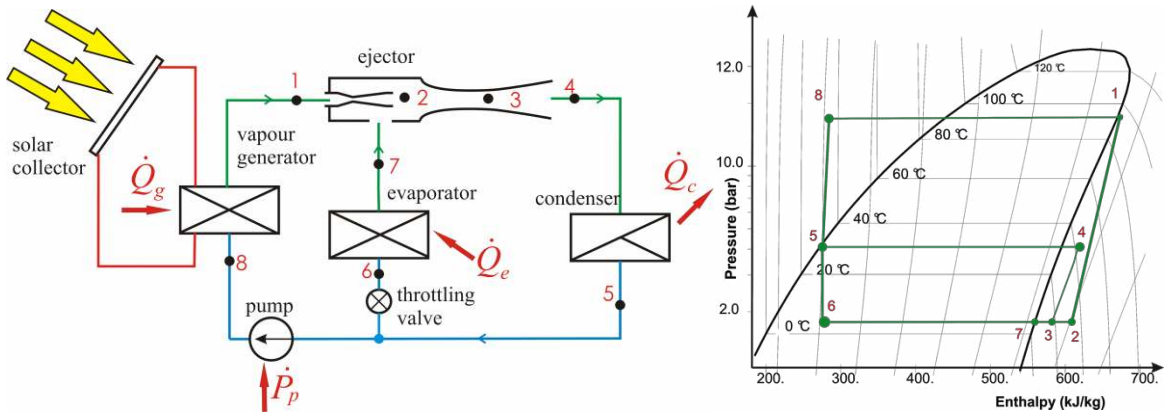

Figure 1. Schematics of the solar cooler (left) and corresponding p-h diagram of thermodynamic cycle

A liquid refrigerant is passed through the pump to the generator (point 8). It is then heated in the generator either by energy from solar panels or waste heat. The first stage of heating produces saturated vapor (point 1), which can be further heated to produce superheated vapor. The vapor enters the motive nozzle of the ejector and undergoes expansion from the generator pressure p_g, to the evaporation pressure p_e (point 2). The ejector sucks vapor flowing from the evaporator (point 7), mixes it with expanded vapor (point 2) with the result being the mixed vapor in state 3. The pressure of the working fluid initially rises slightly as a result of momentum exchange, and then rises more in the diffuser up to the point 4, achieving the condensation pressure p_c. Compressed vapor enters the condenser where

it condenses and may also sub-cool depending on the cooling conditions in the condenser. The working fluid leaves the condenser in the liquid state (point 5). It is then divided into two parts: one part flows to the generator through the small circulating pump. Meanwhile, the remaining part flows through the expansion valve to the evaporator, where it is throttled to the evaporation pressure, p_e, achieving the condition of wet vapor (point 6). Through boiling in the evaporator, the working fluid absorbs cooling capacity, Q_e, from the refrigerant (Bergander, 2015).

2. TEST STAND AND EXPERIMENTAL RESULTS

The schematic of an experimental rig presented in Fig. 2 was designed to operate on isobutane (Butrymowicz et al., 2009). The main elements of the stand are listed in the figure caption. The geometry of the tested ejector is presented in Fig. 3. The motive nozzle throat diameter was D_t= 3.5 mm. Other important factors of ejector geometry are: D_m/D_t = 1.71, L_m/D_t = 23.4, L_d/L_m = 0.84, α_1 = 8° and α_2 = 10°.The testing stand was equipped with the temperature sensors and pressure transducers installed at all locations of interest. The Coriolis mass flow meters with accuracy of 0.15% were used.

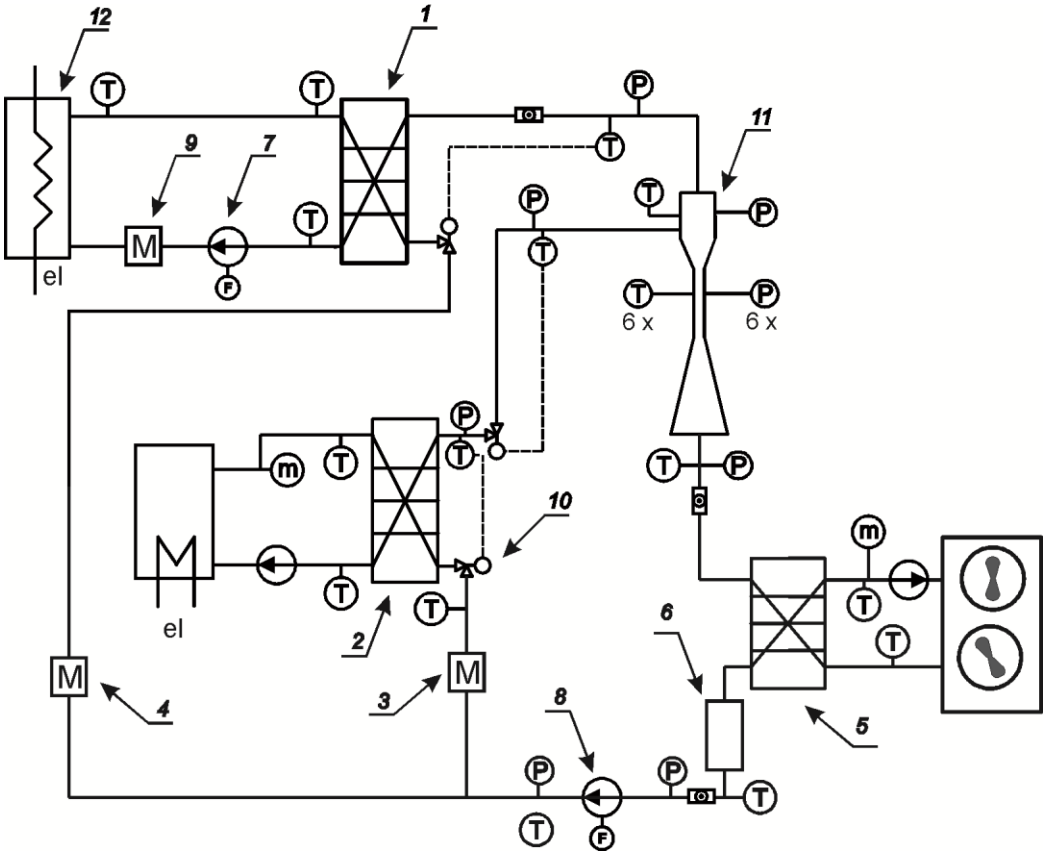

Figure 2. Schematic diagram of testing stand: *1* – vapor generator, *2* – evaporator, 3 – secondary fluid mass flowmeter, 4- primary fluid mass flowmeter, 5 – condenser, 6 – liquid refrigerant storage, 7 - glycol pump, 8 - refrigerant pump, 9 - glycol mass flowmeter, 10 – throttling valve, 11 – ejector, 12 – electrical heater

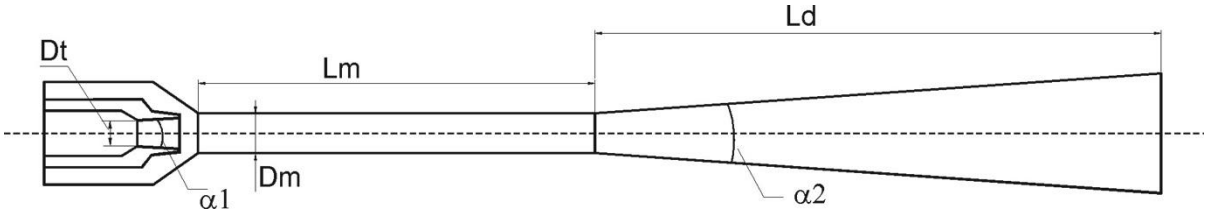

Figure 3 Geometry of the tested ejector.

Sight-glasses were installed at various locations to observe the flow. The test rig was equipped with two additional loops: the first one for the thermal load for the evaporator and another for the condenser cooling. These systems allow for adjusting refrigerant flow rates as well as for changing of operation parameters in wide range. The condenser cooling system was equipped with an automatically controlled dry cooler. The thermal load system was equipped with automatically controlled electrical heater. The stand is also equipped with control valves enabling the adjustment of the operating parameters of the motive vapor at the inlet to the motive nozzle of the ejector. Standard data acquisition facility was used based on commercially available systems. The first one was a real time, Compact FieldPoint system, designed for industrial control. The second was modular SCXI system. This system logs all main parameters and controls valves, pumps, electric heaters and safety system. The computer uses a LabVIEW version 8.6.1 software with additional toolkits. In addition, software dedicated to experimental stand is capable to receive on-line data from software REFPROP, (Lemmon et al. 2013). The real time measurements are shown on the computer screen while all measured data are stored in a data file. During the experiments 100 readings at the steady-state conditions were taken and averaged to make one experimental run, shown in Table 1.

Table 1: Operating parameters of the ejector

Runs	**Unit**	**Run 1**	**Run2**
pressure of motive vapor p_g	MPa	1.27	0.95
superheating of motive vapor ΔT_g	K	10.0	8.0
saturation temperature of motive vapor t_{gs}	°C	77.0	63.7
suction pressure p_e	MPa	0.21	0.20
superheating of suction vapor ΔT_e	K	6.5	5.9
saturation temperature of evaporation t_{es}	°C	9.1	7.0
backpressure p_c	MPa	variable 0.35 – 0.44	variable 0.33 – 0.43
saturation temperature of condensation t_{cs}	°C	variable 25.1 – 33.1	variable 22.8 – 32.0

The experimental investigation were conducted in two runs. The evaporation temperature was kept constant, t_{eI} = 9.1 °C and t_{eII} = 7.0 °C. The condensation temperature was varied between approximately t_c = 23 ÷ 33 °C. The motive stream temperature at saturation condition was set as t_{gI} = 77°Cand t_{gII} = 63.7°C for two runs, respectively.

Superheating of the secondary stream was ΔT_e = 6.5 K for Run No. 1, and ΔT_e = 5.9 K for Run No. 2. Superheating of the motive vapor was ΔT_g = 10 K for Run No. 1, and ΔT_g = 8 K for Run No. 2. The system efficiency COP is calculated as the ratio of the cooling capacity $\dot{Q}_e$ to the thermal energy $\dot{Q}_g$ delivered to the vapor generator and motive power of the mechanical liquid pump *Pp*:

$$COP = \frac{\dot{Q}_e}{\dot{Q}_g + P_p} \tag{1}$$

Motive power of liquid refrigerant pump is calculated as the product of the mass flow rate of refrigerant and the change of the specific enthalpy at the both sides of the pump:

$$P_p = \dot{m}_g \left(h_8 - h_5 \right) \tag{2}$$

In general, the motive power of the refrigerant pump is in most cases very small, usually 1÷2 percent of the thermal energy delivered to the generator and therefore can be omitted. Nevertheless this power was included in present investigations.

Experimental results for both runs are presented in Fig. 4 to Fig.7. Entrainment ratio U is defined as motive to secondary mass flow rates ratio, and compression ratio Π is defined as ratio of the pressure lift produced by the ejector to the difference between motive pressure and suction pressure.

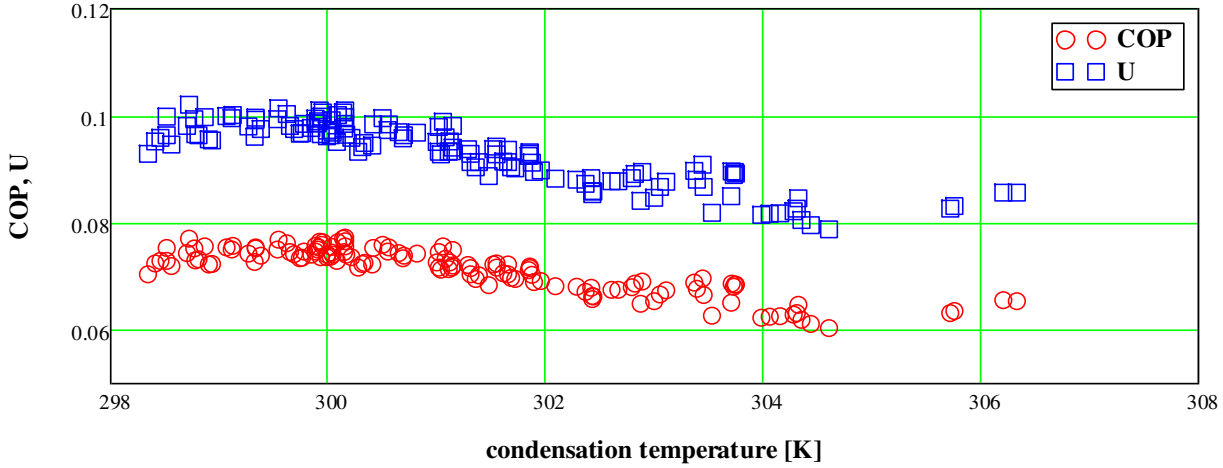

Figure 4. Coefficient of performance and mass entrainment ratio (U) vs. condensation temperature for Run No. 1

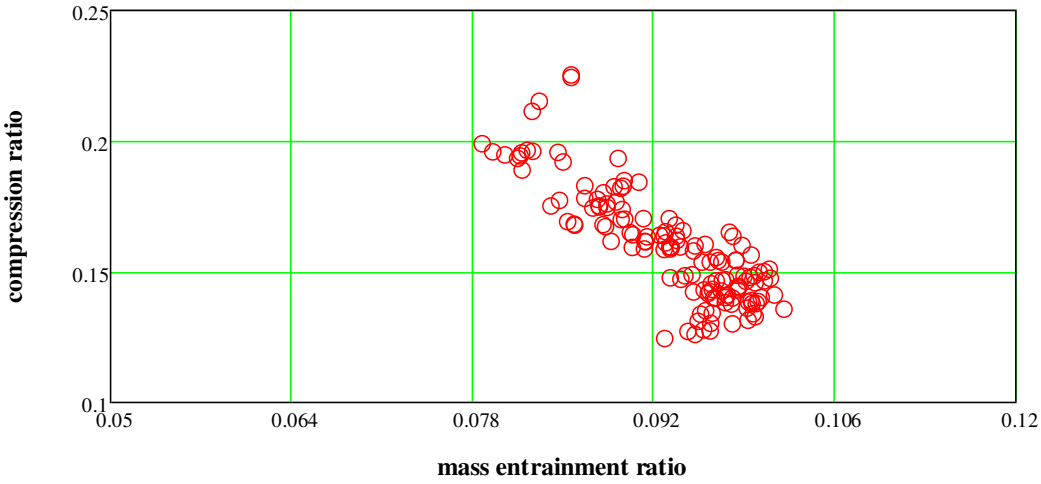

Figure 5. Performance line of the ejector $\Pi = f(U)$ for Run No. 1

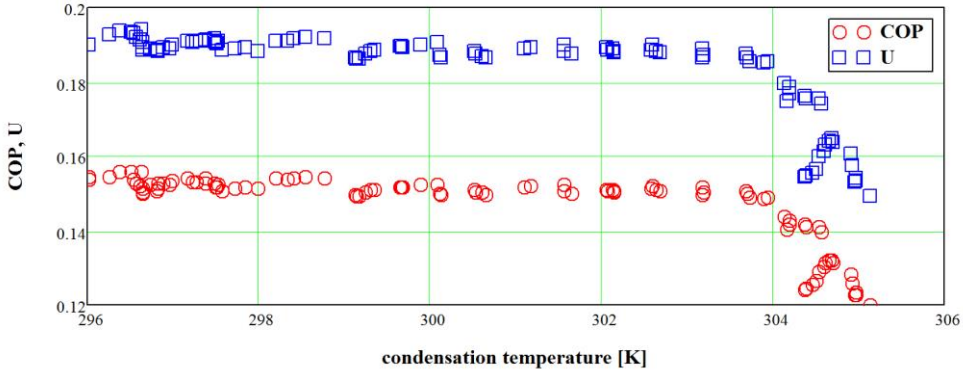

Figure 6. Coefficient of performance (COP) and mass entrainment ratio (U) versus condensation temperature for Run No. 2

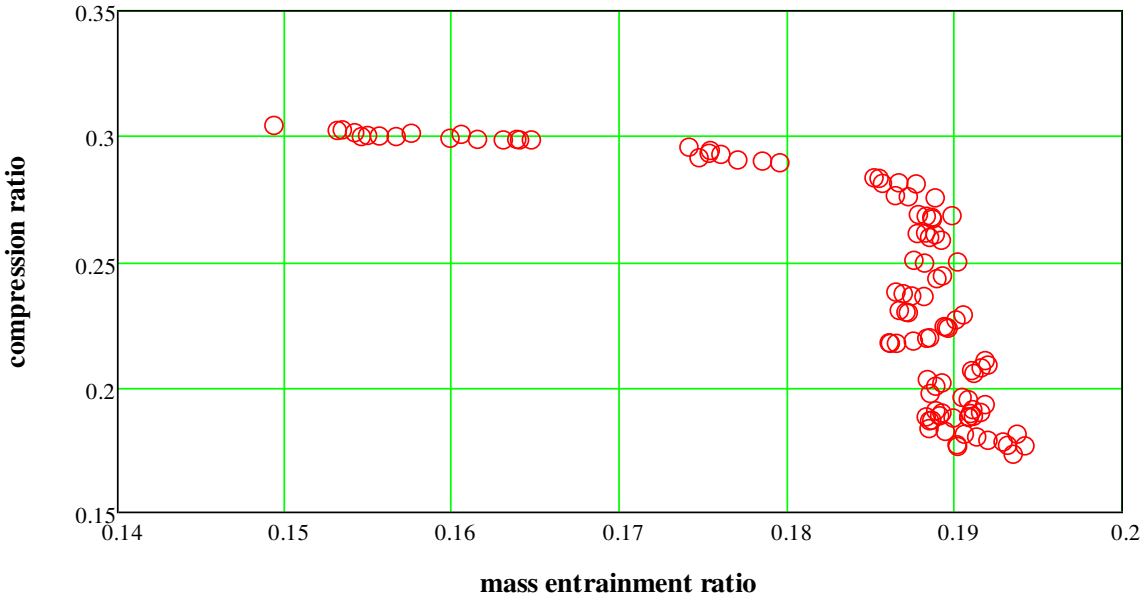

Figure 7. Performance line of the ejector $\Pi = f(U)$ for Run No. 2

Fig. 4 shows COP of the system as a function of condensation temperature for Run No. 1. It can be observed that up to t_c = 28°C , the COP is constant and equal to 0.075 then begins to decrease for higher condensation temperatures. Similarly the mass entrainment ratio (U) shown also in Fig. 4starts to decrease from original value of U = 0.1 when condensation temperature rises above 28 °C. Fig. 5 presents the performance line of the system in co-ordinates: compression ratio Π vs. mass entrainment ratio U. It is seen that Run No. 1 over both on-design and off-design conditions. The ejector operates under on-design conditions when both motive and secondary flows are critical as it is usually assumed in the calculation of the ejector geometry.

Similar results for Run No. 2 are shown in Figures 6 and 7. The COP of the system as a function of condensation temperature shows that at t_c< 30 °C, ejector operates at on-design mode and COP is constant at 0.15 then starts to decrease as condensation temperature rises above 30°C. For on-design operating regime, the mass entrainment ratio is at 0.19 and starts to decrease for condensation temperatures over 30°C. This relationship is illustrated in Fig. 6. The performance line of the system in co-ordinates: compression ratio Π vs. mass entrainment ratio U is presented in Fig 7. It is seen that Run No. 2 covers both on-design and off-design conditions. The maximum reported compression ratio is Π = 0.30 and corresponds to U = 0.15.

3. NUMERICAL MODELING OF MOTIVE EJECTOR

Considering the general goal being experimental verification of the stable operation of the ejector under required operation conditions, the manufacturing of an ejector prototype with required accuracy is essential. For that purpose, special fabrication technology (Kapayeva, 2012 and Usubamatov, 2015) to assure high accuracy and close tolerances was used. In addition, the main goal in this stage of research was the evaluation of the design procedure rather than estimation of the maximum capacity of the ejector. This required CFD calculations for one proposed geometry in order to analyze the operation of the ejector in the whole range of the operation parameters (Smierciew et al., 2010a,b). The compression process by the shock wave should be also analyzed on the basis of the numerical calculations results along with predicted pressure profile produced inside the ejector. The ejector geometry as shown in Fig. 3 was analyzed by means of CFD modeling.

The numerical calculations were carried out with use of ANSYS FLUENT 14. Two numerical models were built, namely:

- 2D axi-symmetric model shown in Fig. 8 that was discretized by means of structural mesh with the density 46 612 cells (48 931nodes);
- 3D model (Fig. 9), discretized by means of structural mesh with the density 42 714 cells (50 800 nodes).

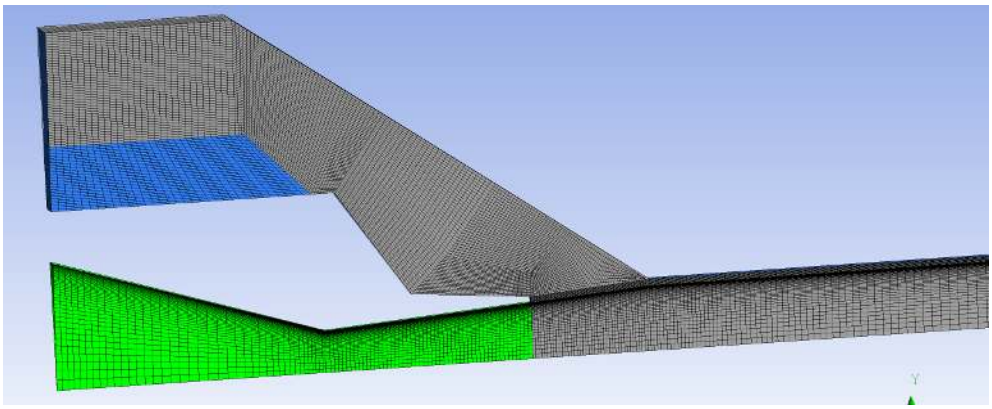

Figure 8. Calculation mesh for the case of the axi-symmetric 2D model of the ejector

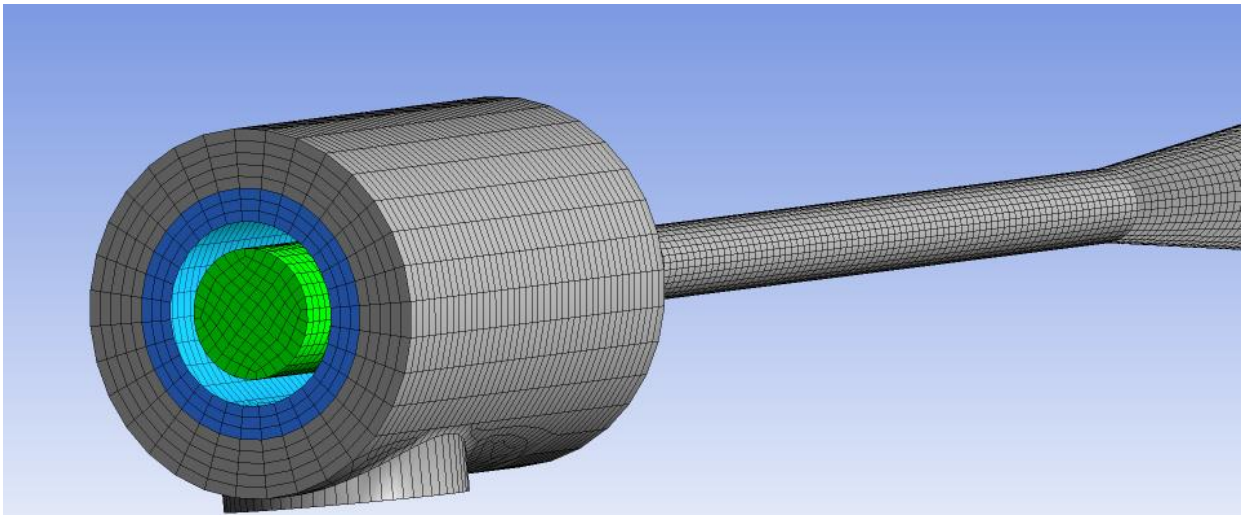

Fig. 9. Calculation mesh for the case of 3D model of the ejector

The numerical calculations were carried out using SST turbulence model that belongs to family of *k-ω* as well as *k-ε realizable* models. The standardized wall function was applied for the case of *k-ε*model along with default model constants for both of the above models. The velocity and pressure distributions were calculated with application of *coupled* algorithm The discretization scheme *second order* of the type *upwind* were chosen. Numerical calculations were carried out for the operating conditions corresponding to the experimental values – specifically the ejector being is powered (motived) with superheated vapor at the average temperature of 60°C.

Calculations results obtained for the case of the axi-symmetric model are presented in Table 2 below while Tables 3 and 4 show the results obtained for 3D model. As seen, the reasonably good agreement between the prediction and experimental data is achieved in terms of the pressure distribution. However, for 3D model, a numerical prediction of mass entrainment ratio is less accurate and this requires further analysis. Note that the accuracy of the mass entrainment prediction is affected also by the measurement error.

Table 2: Numerical predictions compared with experimental data for 2D axi-symmetric model

t_g[°C]	p_g[MPa]	t_e [°C]	p_e[MPa]	p_c [MPa]	m_{gEXP}[kg/s]	m_{gCFD}[kg/s]	m_{eEXP}[kg/s]	m_{eCFD}[kg/s]
58.4	0.689	8.60	0.175	0.340	0.020	0.0231	0.001963	0.00198
60.9	0.736	10.0	0.176	0.340	0.021	0.022	0.004395	0.004378

Table 3: Numerical predictions compared with experimental data for 3D model, Run No. 1

p_{g_exp}	p_{g_CFD} (total/static)		p_{e_exp}	p_{e_CFD}(total/static)		p_{c_exp}	p_{c_CFD}
bar	**bar**		**bar**	**bar**		**Bar**	**bar**
9.4358	9.29	9.15	1.99	1.995	1.99	3.3287	3.3287
t_g [°C]			t_e [°C]			t_c[°C]	
72.1			12.78			53.8	
m_{g_exp} [kg/s]	m_{g_CFD} [kg/s]	$\frac{CFD-EXP}{EXP}\cdot 100\%$	m_{e_exp} [kg/s]	m_{e_CFD} [kg/s]	$\frac{CFD-EXP}{EXP}\cdot 100\%$		
0.027	0.0252	6.707	0.005162	0.0065	-27.7		

Table 4: Numerical predictions compared with experimental data for 3D model, Run No. 2

p_{g_exp}	p_{g_CFD} (total/static)		p_{e_exp}	p_{e_CFD}(total/static)		p_{c_exp}	p_{c_CFD}
bar	**bar**		**bar**	**bar**		**Bar**	**bar**
9.3784	9.187	9.178	1.99	1.995	1.99	3.7529	3.7529
t_g [°C]			t_e [°C]			t_c[°C]	
75.53			12.44			53.99	
m_{g_exp} [kg/s]	m_{g_CFD} [kg/s]	$\frac{CFD-EXP}{EXP}\cdot 100\%$	m_{e_exp} [kg/s]	m_{e_CFD} [kg/s]	$\frac{CFD-EXP}{EXP}\cdot 100\%$		
0.0269	0.0262	2.3175	0.0052	0.0067	-29.3642		

The static pressure distributions along the length of the ejector for two analyzed cases of 3D model are presented in Figures 10 and 11 below. The location of the shock wave compression is clearly visible. Note that the compression in the diffuser may be thought as only a supplementary since vapor compression in the analyzed ejector is obtained mainly by a shock wave. For all CFD calculations, the properties of real vapor were applied according to NIST thermodynamic and thermo-kinetic properties models.

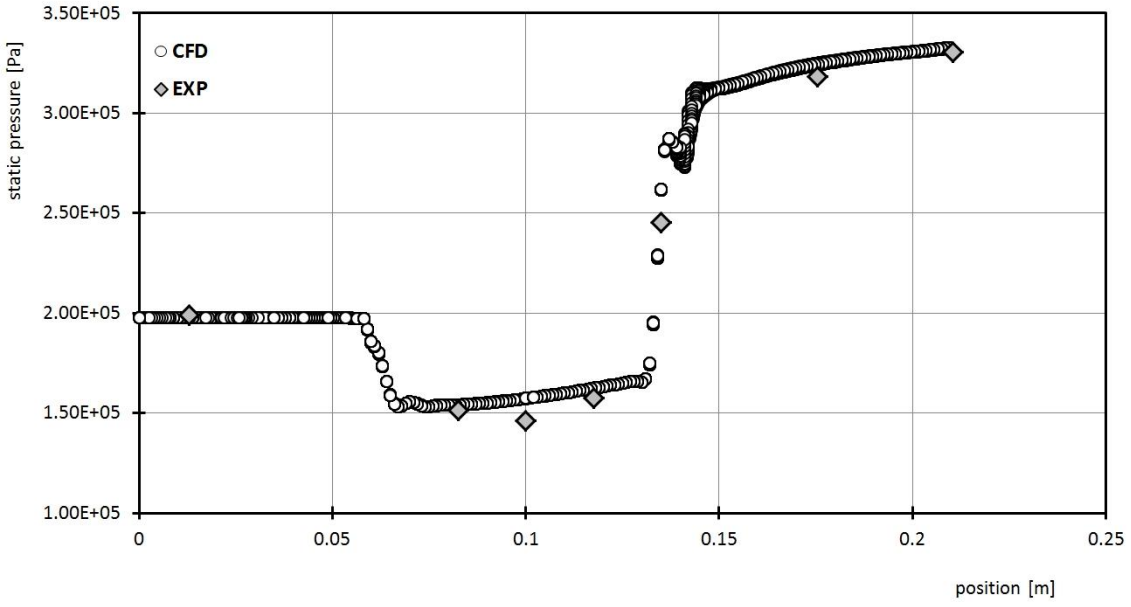

Figure 10. Static pressure distribution on the ejector wall for the test Run No. 1 (see Table 3)

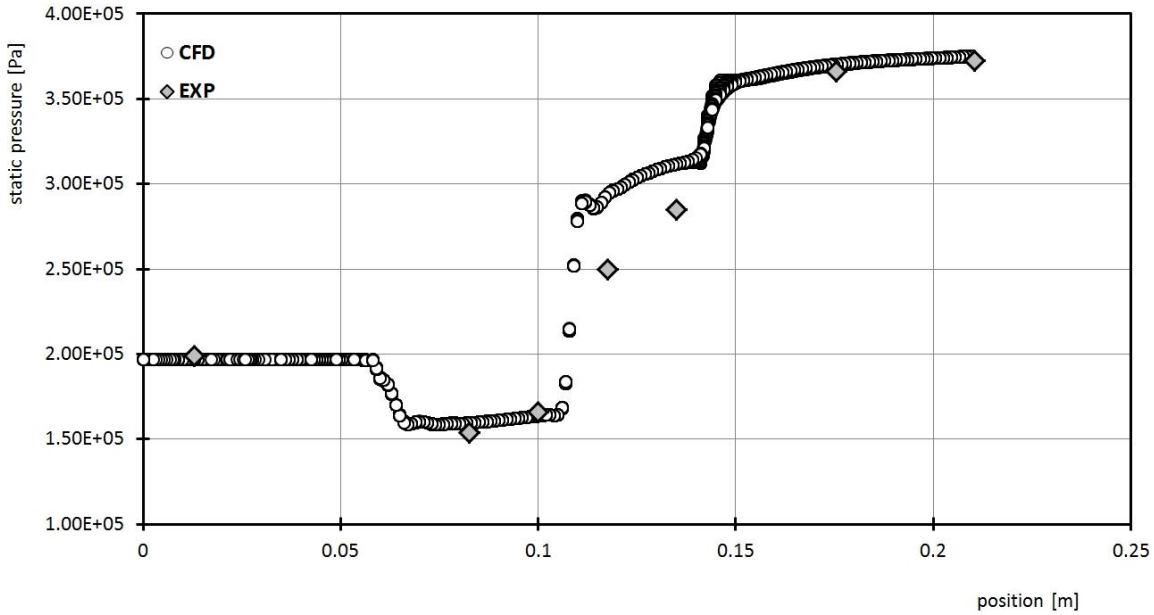

Figure 11. Static pressure distribution on the ejector wall for the test Run No. 2 (see Table 4)

4. PRELIMINARY DESIGN OF SOLAR-DRIVEN COLD STORAGE CHAMBER

As a result of previous cycle modeling (Smierciew et al. 2009), along with presented here CFD analysis of the ejector operation - confirming a reliable ejector operation over wide range of operating conditions -plus systematic experimental investigations, authors were able to perform a preliminary design and component selection for the ejection refrigeration unit. The configuration of the prototype is shown in Figure 12 below. The required surface area of thermal solar collectors for 3 kW of cooling power is approx. 10 m^2. The adequate amount of electric power to drive the liquid pump can be supplied by less than 1 m^2 of photovoltaic panel surface.

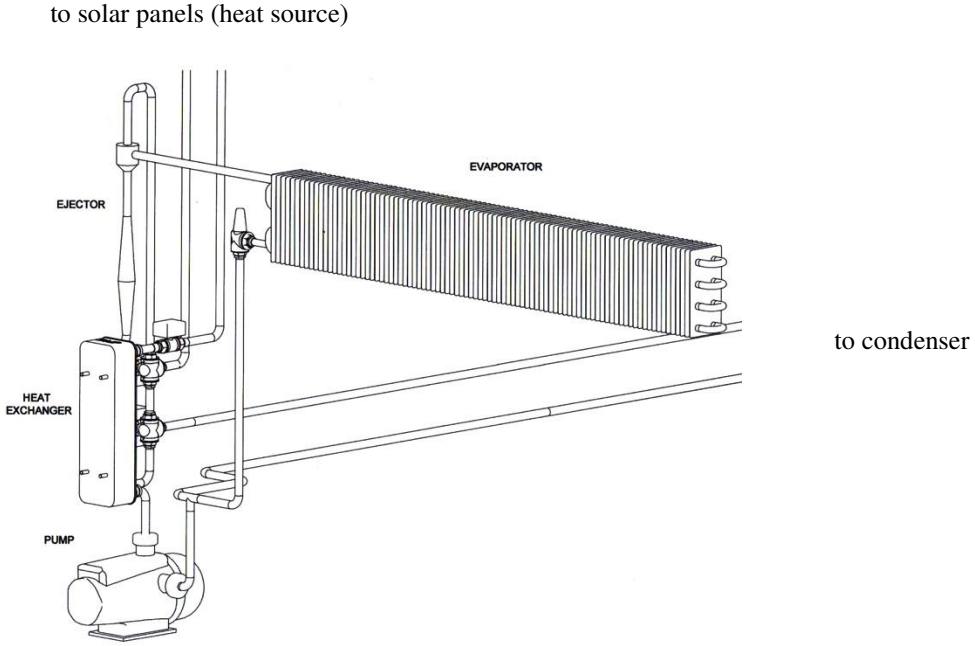

Fig. 12. Configuration of solar cooling system prototype

6. CONCLUSIONS

The described research addresses a refrigeration concept that uses low quality heat (below 100°C), either solar or waste as energy source without need for electricity from power grid and does not pollute the environment. A significant energy saving is realized by a modified thermodynamic cycle that pressurizes liquid instead of vapor. Extensive laboratory tests and CFD modeling were conducted in order to provide the design background for effective cooling system prototype for post-harvest precooling and field storage of fruits and vegetables. There is also a great potential of using this technology for refrigeration and air-conditioning in the Third World countries and in remote areas where electric energy is unavailable. Small solar-based units can be developed for storage of medicines, perishable food, and to cool field clinics.

Significant progress has been achieved in developing a methodology to design ejector geometry capable to adjust the cooling system to varying load conditions. The three-dimensional CFD modeling followed by extensive laboratory experiments had clearly demonstrated a reliable ejector operation under a broad range of changing load and power input. Further, out of many refrigerants under consideration, it was found that isobutane provides highest efficiency and, being a natural substance does not pollute the environment. With technical feasibility being fully confirmed, it can be reasonably expected that an attractive commercial product will emerge.

REFERENCES

Butrymowicz, D., Trela, M., Karwacki, J., Ochrymiuk, T., Smierciew K. (2009). Investigation and modeling of ejector for air-conditioning system, *Archives of Thermodynamics 29* (4), 27-40.

Bergander M., (2015) Ejector Refrigeration Cycles: Classification of Thermodynamic Cycles with Ejectors, *Handbook of Res. on Adv. and Appl. in Refrigerat. Systems and Technologies*, Ch. 1, pp. 1-36, IGI Global 2015,

Gross, K.C., Wang, C.Y., Saltveit, M. (Eds.) (2002) *The Commercial Storage of Fruits, Vegetables, and Florist and Nursery Stocks*, Agricultural Handbook No. 66, USA, Washington DC.

Huang, B.J., Chang, J.M., Wang, C.P., Petrenko, V.A. (1999). A 1-D analysis of ejector performance, *International Journal of Refrigeration 22*, 354–364.

Lemmon, E.W., Huber, M.L., McLinden, M.O., 2013, *NIST Standard Reference Database 23: Reference Fluid Thermodynamic and Transport Properties*-REFPROP, Version 9.1, NIST

Kapayeva S., Komkov M. (2012), The search of the cutting mechanism in the time of sharpening in an atmosphere of the water-soluble polymeric cutting-tool lubricant ВП-4, *B'deshiteizsledovanya",* Vol.33, Sofia, pp. 42-48,

Mizera, G., Butrymowicz, D. 2011.Cold store of new generation for carrot storage, *Proceeding of 23rd International Congress of Refrigeration*, Prague, Paper No. 829.

Mazza, G., 1989, Carrots, in: Eskin N.A.M. (ed.), *Quality and Preservation of Vegetables*, CRC Press, 75-119.

Smierciew, K., Kolodziejczyk, M., Butrymowicz, D. (2010). CFD modelling of ejector operating with isobutane (in Polish), *Technika Chłodnicza i Klimatyzacyjna 17* pp. 434-438.

Smierciew, K, Butrymowicz, D., Karwacki, J., Trela, M., (2009) Modeling of ejection cycle for solar air-conditioning, *Proc. of Int. Seminar on ejector/jet-pump technology*, Louvain-La-Neuve, Belgium, Paper No. 25.

Usubamatov R., Zain, Z.M. Sin T., C, Kapayeva S.D.,(2015) Optimization of multi-tool machining processes with simultaneous action, *Int J Adv Manuf Technol* DOI 10.1007/s00170-015-6920-x, ISSN 0268-3768

ACKNOWLEDGEMENT

This material is based upon work supported by the US Department of Agriculture, under SBIR Phase I Award Number 2014-33610-21919.

DISCLAIMER